Low pressure additive manufacturing of continuous fibre reinforced polymer composites

Heather J. O' Connor[1] and Denis P. Dowling[2]

[1]School of Chemical and Bioprocess Engineering, UCD, Belfield, Dublin 4, Ireland
[2]School of Mechanical and Materials Engineering, UCD, Belfield, Dublin 4, Ireland

*** Correspondence:** Email: heather.oconnor@ucdconnect.ie

Abstract

Continuous fibre reinforced polymer composites have found a wide range of applications in the automotive and aerospace industry, due to their lightweight properties. Recently the use of additive manufacturing (AM) has been developed for the fabrication of these composites. This study investigates the use of both atmospheric and for the first time, low-pressure (1 Pa) processing conditions, for the AM of continuous carbon, glass and Kevlar fibre reinforced nylon composites. DSC was used to compare the thermal properties of the three types of fibre reinforced filament, prior to printing. It was found that the melting peak was dependent on filament type, which can be related to the polymer processing conditions used during their fabrication. Based on computed tomography measurements, it was found that the use of low-pressure printing conditions yielded a reduction in porosity for the carbon, glass and Kevlar printed composites of 5.7, 1.0 and 1.7 % respectively. The mechanical properties of the composites were compared, using a short beam shear test, which assisted in the measurement of interlaminar properties. An increase in interlaminar shear strength of 33, 22 and 12% was obtained for the carbon, glass and Kevlar fibre reinforced polymer composites respectively, when printed under low-pressure, compared with that obtained at atmospheric pressure.

Keywords: Additive manufacturing (AM); 3D Printing; Fibre reinforced polymeric composite (FRPC); Low-pressure; Vacuum

1. Introduction

Fibre reinforced polymeric composites (FRPC) are used in industries such as automotive, marine and aerospace due to their high strength to weight ratio and durability [1]. The composite industry is moving away from traditional labour intensive methods, such as manual layups and are transitioning towards automated composite manufacturing to improve cost efficiency [2]. Examples of which are automated tape layup (ATL), automated fibre placement (AFP) and filament winding (FW).

Additive manufacturing (AM), a process that fabricates parts, layer by layer, from a computer aided design [3], is increasing in popularity in aerospace and various engineering fields, because it offers fast and inexpensive prototyped parts [2]. It encompasses a range of techniques, such as binder jetting, direct metal laser sintering, stereolithography and material extrusion [4]. The focus of this study is on material extrusion, which is the most widely adopted of the techniques. It has previously been referred to by names such as fused filament fabrication (FFF) and the Stratasys trade-marked name, fused deposition modelling (FDM) [5]. Major drawbacks associated with material extrusion are choice of polymer materials and the strength of the printed parts [6]. To address the latter, there is considerable interest in the incorporation of additives as a reinforcement phase into the printed parts [6-8]. Examples of additives are glass, carbon and metal chopped fibres and powders. Zhong et al. [6], for example demonstrated that reinforcing ABS filament with chopped glass fibres yielded an increase in part tensile strength, with a reduction in flexibility. A similar result was obtained with chopped carbon fibre [7], as well as with metal particles [8]. In addition to particle reinforcements, there have been a number of reports on the incorporation of continuous fibres into the polymer matrix [9-12].

There are two approaches to printing polymers, reinforced with continuous fibres. The first involves merging the fibre bundle and polymer filament during the printing process. This has also been referred to as 'in situ-fusion' [12] and a number of authors have proposed variations of this printing method [11,13-15]. Matsuzaki et al. [13] were one of the first to report on printing continuous fibre reinforced polymers. They investigated printing carbon fibre and twisted yarns of natural jute fibre with PLA, their mechanical properties were compared with that of the polymer. Hao et al. [11] printed continuous carbon fibre epoxy laminates as well as grid structures. The raw carbon fibre bundles were passed through an epoxy resin pool, before entering the heated print head. The fabricated parts were then cured in a high temperature oven. The resulting composites were shown to outperform similar thermoplastic composites.

The second approach involves fabricating a fibre infused polymer filament, which is also referred to as pre-impregnated filament (prepreg) [12]. This filament is then extruded using the same operating principle as applied in conventional AM material extrusion. In studies performed by Hu et al. [16], PLA filament reinforced with carbon fibre was manufactured. This was used to print continuous FRPC, using a

modified polymer extrusion head. Examples of other printed fibre reinforced composites is the work of Tian et al. [14], who produced laminates by simultaneously feeding carbon fibre and PLA through the print head. While Bettini et al. [15], modified a standard extrusion head of an FDM printer to facilitate the processing of aramid fibres interspersed in a PLA matrix.

A variation of this 'prepreg' AM method was commercialised in 2014 by Markforged, who developed printers which utilise continuous carbon, glass and Kevlar prepreg nylon filament, with 35 – 41 % fibre volume [12,17]. These printers print pre-impregnated (prepreg) fibre filament, into a nylon polymer matrix, using a dual extrusion head system. The performance of the resultant composite parts has been extensively evaluated [9,10,12,18-23]. Dickson et al. [10], compared the tensile and flexural properties of carbon, glass and Kevlar fibres using both a concentric and isotropic fibre pattern. Likewise, Justo and Távara [18], detailed the tensile and compressive properties of carbon and glass printed samples and compared them with traditional epoxy laminates. While Caminero et al. [9] investigated the effects of layer thickness and fibre content on the interlaminar shear strength of printed carbon, glass and Kevlar parts. Melenka et al. [23], focused on Kevlar printed nylon composites, proposing a model that allows the tensile properties of fibre reinforced 3D printed parts to be predicted.

One major concern, affecting the efficient use of 3D printed continuous FRPC's are their weak interlaminar bonding performance [9]. A factor influencing this is the presence of voids or porosity in the as-deposited layers. Many conventional composite processing techniques are carried out under low pressure conditions, as in a vacuum bag [24], or using a pressure differential such as autoclave [25] to reduce void formation in the fabricated composites. In a previous study, low-pressure printing conditions of 1 Pa were evaluated on the physical and mechanical properties of three polymers. A reduction in porosity of 55% and a tensile strength increase of 42% was observed for printed nylon parts [26]. It was proposed that during low-pressure printing conditions, that there was a reduction in the heat dissipated during the printing process. This enabled the polymer layers to achieve enhanced molecular diffusion, which is thermally driven and resulted in increased bonding performance, as well as a reduction in the accumulation of residual stress.

In this paper for the first time, the printing of continuous fibre reinforced polymer composites under low-pressure conditions is investigated. The study includes an evaluation on the effect on composite microstructure and interlaminar bonding performance, when printed under both atmospheric and low-pressure conditions.

2. Experimental

- *Materials, printer and specimen preparation*

Pre-impregnated (prepreg) continuous fibre filaments of carbon, glass and Kevlar were obtained from Markforged. These three filaments consist of the continuous fibre, infused with nylon and no additional nylon was added during the printing process. Each filament was used to fabricate composite layers with 35 – 41% fibre volume fraction [12,17]. The printing study was carried out inside a steel vacuum chamber, with an internal diameter of 45 cm and a height of 50 cm, operating either at atmospheric pressure or low pressure (1 Pa), as seen in Figure 1. The chamber was pumped down using a rotary and roots pumping system and the pressure during printing was maintained at 1 Pa and monitored using an Edwards Active Gauge Controller. The parts were fabricated using a Monoprice Select Mini 3D Printer V1 system, chosen based on its dimensions of 343 x 287 x 190 mm, with a build area of 120 x 120 x 120 mm, which allowed it to fit inside the vacuum chamber. A Markforged 0.6 mm nozzle, designed for the filament, was used to facilitate the printing. A delay in the print of 120 seconds was added in advance of printing, to allow the chamber to reach a stable pressure of 1 Pa. Each test specimen took 22 minutes to complete and the chamber was brought back to atmospheric conditions, approximately 30 seconds after each print was finished. The initial print parameters chosen were based on the manufacturers recommendations for the filament using a MarkOne printer and modified to yield the most consistent and low porosity print. Table 1 details the final print parameters.

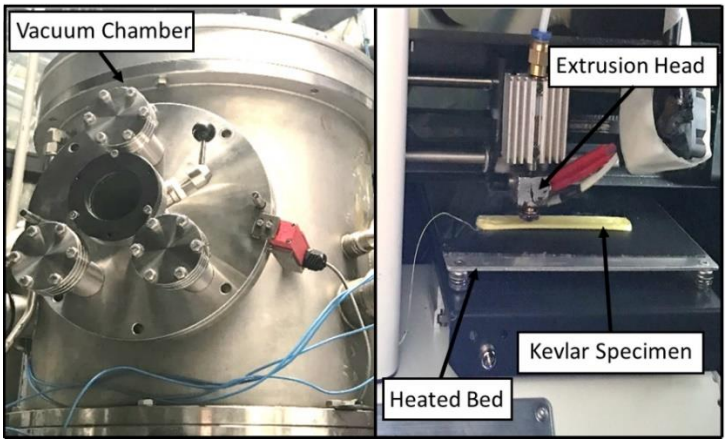

Figure 1: *Left*: vacuum chamber inside which the parts were printed, *Right*: printer arrangement inside the chamber showing the extrusion head used to print Kevlar reinforced PA on a heated bed.

The strength of the printed composite and the fibre-matrix bond was determined using an interlaminar shear (ILS) test. The methodology described in ASTM D 2344 [27], was used to examine the mechanical

performance of the printed composites, as there is no standard test method for the shear properties of 3D printed continuous FRPC. The dimensions of the ILS specimen were selected such that the length is thickness × 6, the span for testing is thickness × 4 and the width is thickness × 2. A CAD file with the dimensions of 10 × 2 × 50 mm was created on Autodesk and exported as a an STL file. Repetier Host V2.1.3 was used to slice the STL file using the print parameters as detailed in Table 1. The sample pattern chosen was the concentric fibre pattern as seen in Figure 2, which illustrates the area used for sample extraction, producing two specimens with a unidirectional pattern (0°), which were then cut to produce two samples of 12 × 4 × 2 mm.

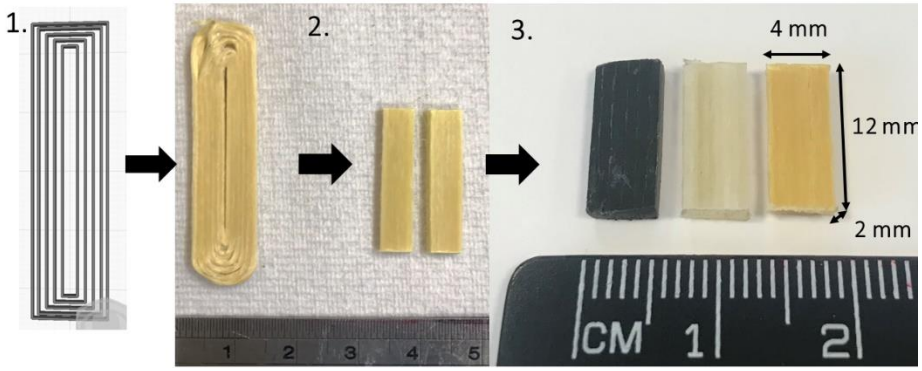

Figure 2: Image 1 shows a concentric fibre pattern from the STL slicing software, Image 2 exhibits a photograph of a printed Kevlar as well as sectioned parts and Image 3 shows the carbon, glass and Kevlar printed ILSS test specimens, respectively.

Table 1: 3D Print Parameters

	Filament diameter (mm)	**Layer height (mm)**	**Track width (mm)**	**Layer Count**	**Speed (mm/s)**	**Nozzle Temperature (°C)**	**Bed Temperature (°C)**
Carbon	0.37	0.125	0.6	16	8	250	60
Glass	0.30	0.11	0.6	18	8	250	60
Kevlar	0.30	0.11	0.6	18	8	250	60

- *Characterisation*

The thermal properties of the 'prepreg' filaments were evaluated using differential scanning calorimetry (DSC) on the as received filament. The nylon infused, continuous fibre filament was heated to 300°C and cooled to -20°C at a rate of 10 K min^{-1}, using a Netzsch DSC214, under a 40 mm / min nitrogen atmosphere. The glass transition temperature (T_g) was evaluated according to the half-step method. The

percentage crystallinity, $X_{m,}$ was calculated using equation 1 [28], where the enthalpy of fusion, ΔH_m, was obtained by integrating the melting peak. The heat of fusion of 100% crystalline polyamide 6 (nylon), ΔH_m^0, was taken as 176 J g^{-1} [29]. Analysis of the peaks was performed using Proteus evaluation software.

$$X_m = \frac{\Delta H_m}{\Delta H_m^0} \times 100 \qquad \text{Equation 1}$$

The print morphology was examined using an Olympus Gx51 Inverted Metallurgical Microscope and a Tabletop Hitachi tm 1000 SEM. The thickness, length and breadth were recorded using a digital vernier callipers, Digi Plus-Line supplied by Vogel Germany GmbH & Co.KG. Preliminary printing studies were carried out in order to optimise the material properties of the composites. The optimised parts were evaluated, and the results are presented in this paper. The materials evaluation was based on 5 test specimens (12 × 4 × 2 mm) per sample set (carbon, glass and Kevlar).

X-ray micro Computed Tomography (μCT) was used to analyse the prints internally in order to evaluate the level of porosity. The test samples were stacked and mounted in the μCT chamber using Styrofoam, due to its low density. A maximum X-ray energy of 90 kV and 80 μA was used to scan each composite stack on a GE Nanotom m X-ray μCT scanner (GE Sensing & Inspection Technologies GmbH, Wunstorf, Germany). A total of 1200 projection images were acquired during a 9-minute scan with a resolution of between 8 - 10 μm. The projection images were reconstructed to produce volumetric data using the software datos|rec (GE Sensing & Inspection Technologies GmbH, Wunstorf, Germany). The μCT volumes were then visualised using VG StudioMAX® 3.1.2 (Volume Graphics GmbH, Heidelberg, Germany). Image stacks (16 bit) were exported from this software. Using these image stacks, 20 images per sample were converted to 8 bit and passed through a thresholding filter, to facilitate the estimation of the percentage ratio of voids in the printed parts (black area representing air in contrast to the grey polymer and fibre). The mean porosity of each composite type printed under atmospheric conditions and low pressure were compared using a two-sample t-test [30]. The probability of significance P, with a threshold of ($P<0.05$), corresponding to a 95% confidence limit, was calculated and is used as a measure of significance, in this study.

- *Mechanical performance*

The interlaminar shear strength (ILSS), also referred to as short beam shear (SBS) testing was carried out according to ASTM D 2344 [27] and was used as a comparative test method, to investigate the influence of low-pressure printing conditions. Each sample set consisted of at least 10 specimens and

the tests were carried out room temperature. The shear properties were measured using a three-point bend test configuration on a Tinius-Olsen (US) Hounsfield 50 K screw-driven tensile test machine at a speed of 1 mm / min and a 10 kN load cell. The interlaminar shear strength τ, expressed in MPa, is calculated according to equation 2. Where P_m is the failure, or maximum load observed during the test (N), b is the width of the specimen (mm) and h is the thickness (mm), of the specimen.

$$\tau_{ILSS} = 0.75 \times \frac{P_m}{b \times h} \qquad \text{Equation 2}$$

The mean SBS strength of the composites printed under atmospheric conditions and low pressure conditions were compared using a simple two sample t-test [30]. The significance P, with a threshold of ($P<0.05$), corresponding to a 95% confidence limit, was calculated and is used as a measure of significance.

3. Results and Discussion

- *Filament characterisation*

Prior to printing, the carbon, glass and Kevlar nylon filaments used were examined using SEM. The micrographs given in Figure 3 depicts a single piece of each of the carbon, glass and Kevlar fibre / nylon filament, illustrating the continuous fibres, surrounded by the nylon polymer.

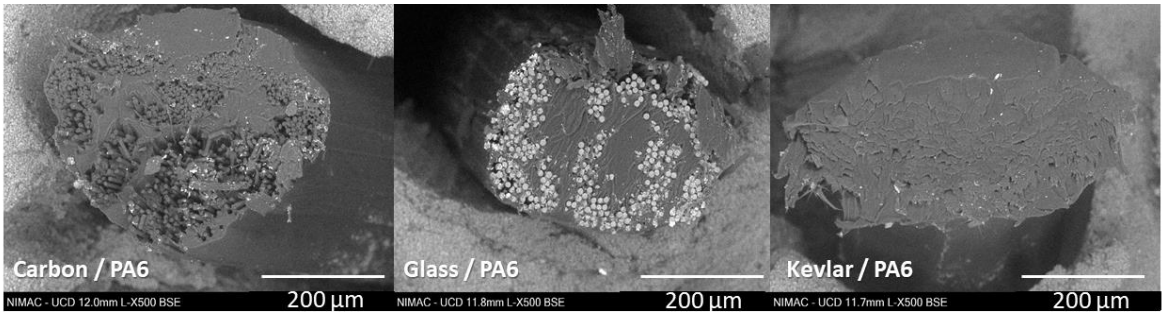

Figure 3: Micrograph of the as-received carbon, glass and Kevlar fibres / nylon filaments. Note that comparing these three images that the carbon and Kevlar fibres due to their high carbon content are not as clearly visible as the glass fibres.

The thermal properties of the three fibre reinforced filaments were evaluated using DSC measurements. Table 2 details the glass transition temperatures (T_g), the melting peak (T_m), the melting enthalpy (ΔH_m) and the calculated percentage crystallinity (X_m), obtained from the heating and cooling cycles. For all three reinforced filaments, a broad flat peak between 70 – 140 °C was observed in the first heating DSC thermogram. This was due to the evaporation of low concentrations of moisture adsorbed on the nylon filament. This peak was more noticeable for the Kevlar reinforced filament, indicating a higher level of moisture present. The moisture evaporation fits well with the shift in the glass transition temperatures of 10 and 9 °C, observed between the first and second heating cycle, of the glass and Kevlar filament. A typical thermogram for the heating and cooling cycles of the glass fibre / nylon filament is given in Figure 4. Note, the second heating is represented by the dotted line which is stacked below the first heating cycle for clarity. In the case of the glass and Kevlar filament, both exhibit a single broad melting peak at 202 °C in the first heating, a sharp crystallisation peak at 159 °C during the cooling stage, followed by broad double structured endotherm in the second heating at 195 and 202 °C approximately, as seen in Figure 4 and more closely examined in Figure 5. The double structed melting peak indicates two melting phases observed in the second heating.

In the case of the carbon fibre / nylon filament, the melting peak was found to be absent, this was in contrast with what was observed for glass and Kevlar filaments. Previous authors have highlighted that the shape and size of the melting peaks observed in DSC are dependent on the thermal history of the nylon polymer [31]. Indeed, it is reported that when the polymer was exposed to 250°C for 30 hours that the melting peak was absent. This would indicate that during the fabrication of the carbon fibre / nylon filament that the polymer may have been exposed to relatively high temperature, in contrast to that used during the processing of the glass and Kevlar fibre / nylon filaments, for which the melting peak is present.

Table 2: Glass transition temperatures (T_g), the melting peak (T_m), the melting enthalpy (ΔH_m) and the percentage crystallinity (X_m) of the carbon, glass and Kevlar / nylon filament, obtained – averaged from three measurements.

Filament Type	**1st heating**				**Cooling**			**2nd heating**			
	T_g (°C)	T_m (°C)	ΔH_m (J/g)	X_m (%)	T_c (°C)	ΔH_c (J/g)	X_c (%)	T_g (°C)	T_m (°C)	ΔH_m (J/g)	X_m (%)
Carbon / Nylon	68	-	-	-	-	-	-	-	-		-
Glass / Nylon	59	202	20.8	11.8	159	20.1	11.4	49	202	17.5	9.9
Kevlar / Nylon	56	202	23.5	13.3	159	22.4	12.7	47	201	20.8	11.8

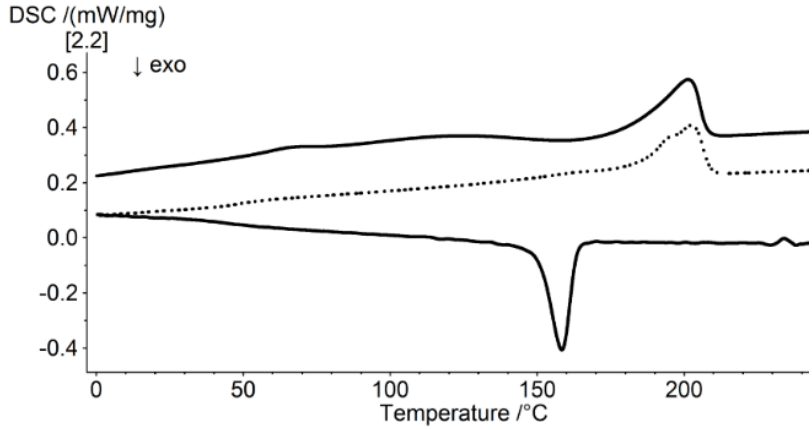

Figure 4: A typical DSC thermogram of the glass fibre / nylon filament, exhibiting the first heating and cooling cycle (solid line) and the second heating is stacked below the first heating cycle, represented by a dotted line.

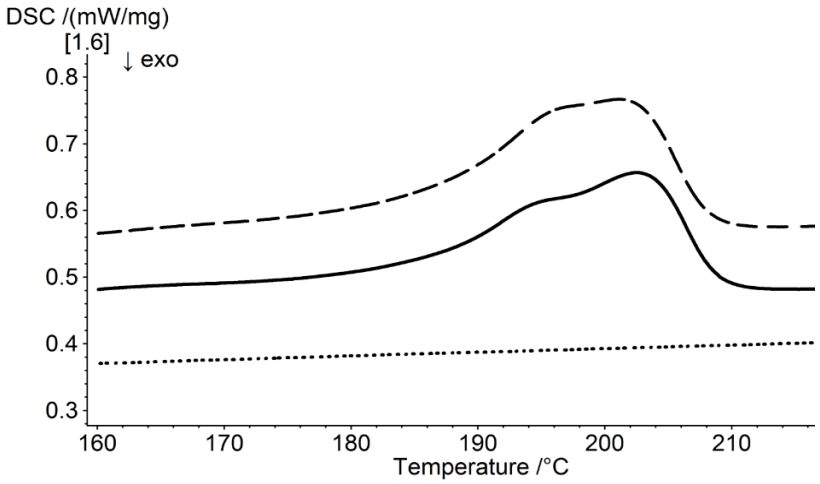

Figure 5: Comparison of the melting peak, observed in the second heating of Kevlar fibre / nylon (dashed line), glass fibre / nylon (solid line) and the absence of the melting peak in the carbon fibre / nylon (dotted line).

- *Microscopy evaluation*

In this section, the results of the SEM examination of the printed composites obtained under both pressures' conditions are compared. Visual examination clearly indicates a reduction in porosity for the carbon FRPC specimens when printed under low pressure. The porosity in the glass and Kevlar samples fabricated under both printing conditions, could not be clearly estimated using SEM. The micrographs in Figure 6, compare an area of the cross sections of carbon FRPC printed under both atmospheric and low-pressure printing conditions. A high level of porosity and poor fibre impregnation is observed in the part printed under atmospheric conditions (A). It was noticeable from the SEM images that porosity was present both between the fibres within the individual filaments, as well as between the printed

filaments. The part printed under low-pressure (B), exhibits a significant reduction in porosity, in addition to reduced fibre matrix separation. Micro CT scans (μCT) were used to quantify the porosity within the composites.

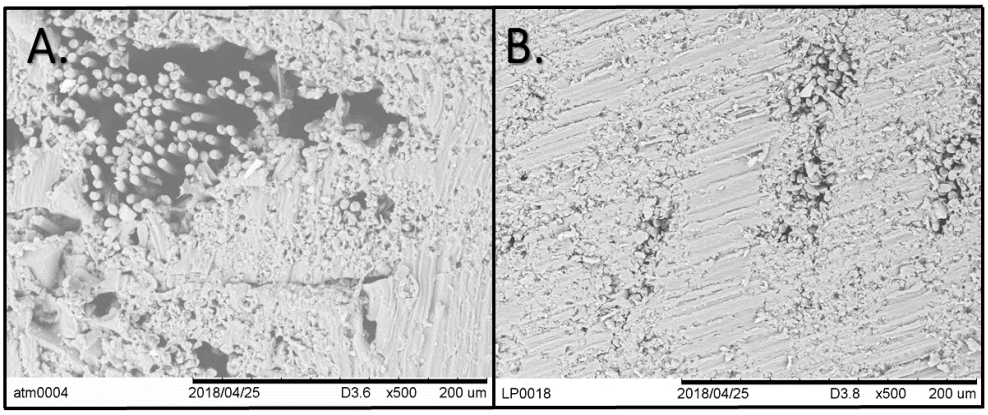

Figure 6: SEM micrographs comparing the porosity observed in cross sections of carbon fibre nylon composite printed under atmospheric conditions (A.) and at low-pressure (B.)

- *Computed tomography*

Prior to mechanical testing, five specimens from each sample set were scanned and their porosity was calculated. In the case of all three fibre types, a reduction in porosity was observed in the composite parts printed under low-pressure, in comparison to those printed under atmospheric. Table 3 details the average porosity obtained under both pressure regimes and the corresponding P value. The carbon FRPC saw the largest decrease from 6.8 to 1.1%, which is an 84% decrease in the porosity, when compared to that obtained using atmospheric processing conditions. The corresponding porosity reductions for glass and Kevlar FRPC's were 69% and 70% respectively.

Table 3: The calculated carbon, glass and Kevlar FRPC porosity's, using micro CT scans

Fibre	Printing Condition	Porosity (%)	P-value
Carbon	Atmospheric	6.8 ± 1.6	< 0.000
	Low-pressure	1.1 ± 0.5	
Glass	Atmospheric	1.5 ± 0.2	< 0.000
	Low-pressure	0.5 ± 0.2	
Kevlar	Atmospheric	2.5 ± 0.9	< 0.005
	Low-pressure	0.8 ± 0.2	

Figure 7 provides an example of two 2D μCT images taken of printed carbon FRPC. Comparing the composite specimen obtained under atmospheric conditions (A) with that obtained under low pressure (B), it is clear that the former has a much higher concentration of darker regions, which is directly correlated to porosity. Note that while this porosity can be seen throughout the sample, it is primarily present along the interface of each print track, indicating poor polymer bonding of the layers.

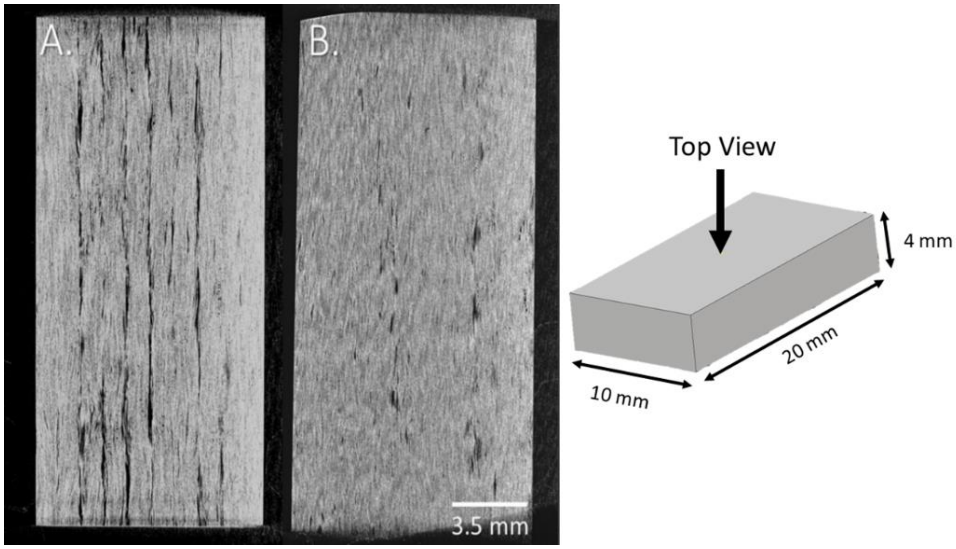

Figure 7: 2D μCT scan images of A. carbon FRPC printed under atmospheric conditions and B. under low pressure. The dark regions are associated with porosity. The schematic on the right illustrates the direction of the cross section of the scan.

Figure 8 illustrates a 2D, front view cross section of the Kevlar FRPC, printed under atmospheric pressure (A) and low-pressure (B). A detailed examination of the voids in the specimens printed under atmospheric pressure, demonstrates that they exhibit an irregular shape and that they occur from the separation at the compressive sides of the deposited track - example of which is labelled 1 in Figure 8. These large void areas are not observed for the composite printed under low-pressure. Individual tracks and layers are also observed, indicating incomplete bonding at the polymer interface, when printed under atmospheric conditions – area 2. Again, these tracks are difficult to observe in the specimen printed under low-pressure. Note that for both the atmospheric and low-pressure prints, small areas of porosity, associated with incomplete impregnation of the fibre bundles by the nylon matrix, are observed. A similar trend is observed in the glass FRPC, printed under both pressure regimes.

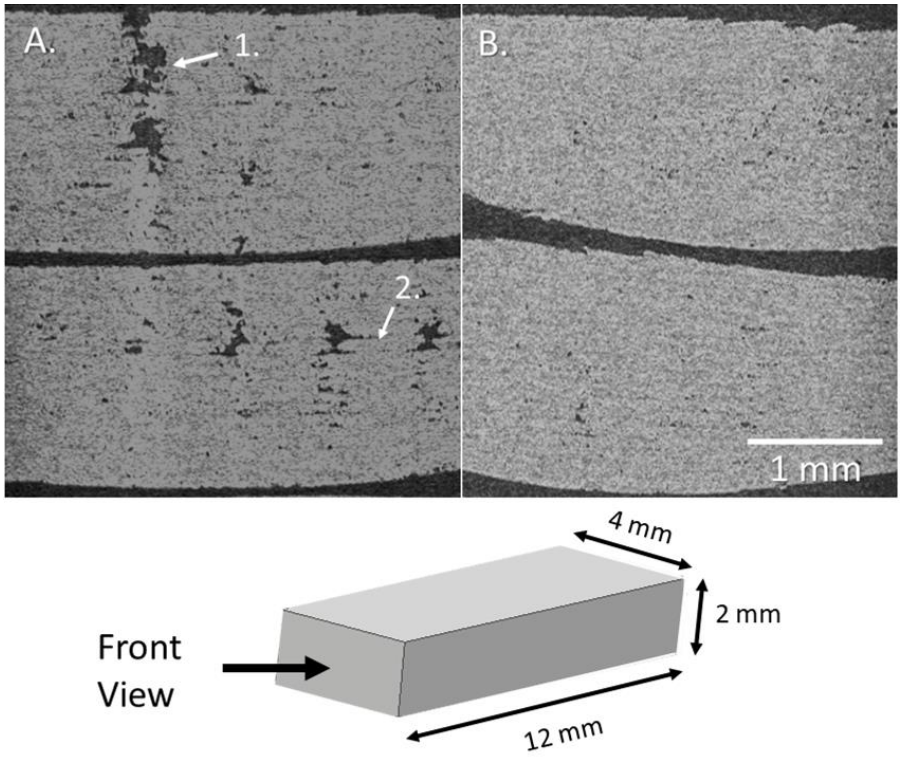

Figure 8: 2D images exported from μCT image stacks, comparing Kevlar FRPC printed under atmospheric conditions (A) and low-pressure conditions (B). The schematic at the bottom illustrates the direction of the cross section of the scan.

The bonding of the polymer layers, during printing is usually described in two steps; the first is surface contact and the second molecular diffusion, which is thermally driven [32]. During polymer extrusion printing, under standard atmospheric conditions, heat is quickly dissipated through convection and forced conduction and the polymer layer rapidly solidifies, often leading to poor layer adhesion and high porosity. During low-pressure printing conditions, heat is largely dissipated only by conduction and rate of heat loss is greatly reduced [26]. Enhanced bonding between polymer layers (an increase in molecular diffusion) occurs when the temperature of the part remains above its glass transition temperature. In this study, the polymer and continuous fibre filament are printed under low pressure for the first time. The low-pressure conditions resulted in a reduction in heat loss and this is thought to facilitate the nylon polymer matrix to maintain a temperature close to its glass transition temperature of 47 - 68°C, thus facilitating enhanced molecular diffusion and bonding between the layers. The resultant parts, in comparison to those printed under atmospheric pressure, exhibited a significant decrease in porosity and enhanced interlaminar bonding. Therefore, the significant reduction in porosity in the continuous FRPC's printed under low-pressure conditions, in contrast to those printing under atmospheric conditions, is likely to be due to the combination of the reduced air entrainment during the low-pressure printing, combined with the retention of heat in the composite associated with the low-pressure environment.

- *Interlaminar shear strength*

To investigate the effect of low-pressure printing conditions on the mechanical strength of continuous FRPC, a short beam shear test was carried out. The adhesion between the fibre and polymer matrix is one of the main factors that determines the strength of a FRPC [9]. Table 4 details the average maximum loading force and the obtained ILSS values. The mechanical strength of the part is dependent on fibre type: Carbon > Glass > Kevlar [10]. It was found that low-pressure printing conditions, exhibited a significantly higher ILSS value, for each of the fibre types. The carbon FRPC printed under low-pressure exhibited the highest strength of 58 MPa, 33% higher than that, printed under atmospheric conditions. The mechanical strength of the glass and Kevlar FRPC increased by 22% and 12% respectively. This enhanced mechanical strength obtained for parts printed under reduced pressure is attributed directly to the reduction in porosity.

Table 4: The interlaminar shear strength (ILSS) of continuous carbon, glass and Kevlar RPC, printed under both atmospheric and low-pressure conditions.

Fibre	**Printing Condition**	**Force (N)**	**ILSS (MPa)**	**P value**
Carbon	Atmospheric	575 ± 122	43 ± 7.4	< 0.000
	Low-pressure	759 ± 72	58 ± 5.2	
Glass	Atmospheric	522 ± 41	39 ± 3.4	< 0.001
	Low-pressure	643 ± 78	48 ± 5.6	
Kevlar	Atmospheric	390 ± 18	28 ± 2.0	< 0.001
	Low-pressure	423 ± 20	32 ± 1.3	

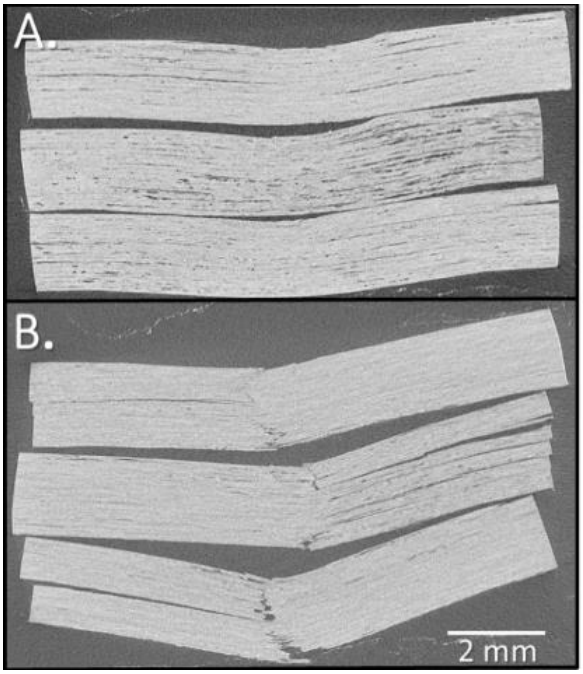

Figure 9: A comparison of μCT scans of carbon specimens after ILSS testing. Image A is the carbon FRPC printed under atmospheric pressure and illustrates minor interlaminar shear failure. Image B is the carbon FRPC printed under low- pressure and depicts multiple shear failure.

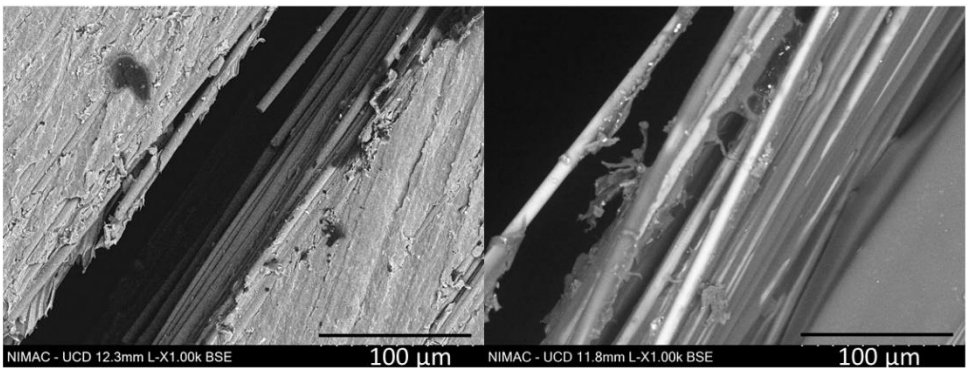

Figure 10: SEM micrographs of carbon (left) and glass (right) FRPC printed under low-pressure conditions, depicting interfacial and cohesive failure respectively.

Micro CT scans were used to examine the failure modes of the ILSS test specimens, according to ASTM D 2344 [27]. In the case of the glass and Kevlar prints, the failure modes were primarily inelastic deformation under atmospheric conditions and a combination of inelastic deformation with some interlaminar shear failure, under low-pressure conditions. It was observed between the two printing regimes, that the parts printed under low-pressure, retained the deformation from the 3-point test configuration more so than the parts printed under atmospheric conditions – indicating a lower elasticity in the parts printed under low-pressure. The carbon reinforced specimens, printed under atmospheric conditions, exhibits interlaminar shear failure with some inelastic deformation, (Figure 9, *A*). In

contrast, those printed under low pressure exhibits multiple interlaminar shear failure and some flexural failure is also observed (Figure 9, *B*). SEM micrographs of the carbon FRPC (Figure 10, *left*) and the glass FRPC (Figure 10, *right*) printed under low pressure conditions, further illustrates the interlaminar shear failure and the fibre matrix separation. The carbon reinforced specimens exhibit interfacial failure under both low and atmospheric pressure. In the case of the glass and Kevlar, extreme fibre – matrix separation was not observed, and the printed parts exhibited primarily cohesive failure under both printing pressures.

Table 5 details the ILSS values obtained in this study, alongside AM fabricated continuous carbon, glass and Kevlar fibre nylon composites, published in a study by Caminero et al. [9], using the same prepreg filaments. They obtained ILSS values of 32, 30 and 14 MPa for the carbon, glass and Kevlar composites, respectively. These are lower than the values obtained in the present study of 43, 39 and 28 MPa printed under atmospheric pressure and 58, 48 and 32 MPa when printed under low-pressure conditions. These differences are likely to be associated with the print parameters used, in addition to the difference in fibre volume fraction. The AM printed composite parts were also benchmarked against an industrial carbon fibre epoxy laminate from Hexcel, fabricated via autoclave, as an example of an industry standard composite. Taking the example of the shear strength of 105 MPa reported for a carbon fibre epoxy, which is widely used commercially, the values obtained of 58 MPa for the carbon fibre nylon composite are clearly significantly lower. As expected, the thermoset resin exhibits significantly higher mechanical performance, compared with nylon. It is clear therefore that while the low-pressure printing conditions yield an improvement in the mechanical performance, significant further research will be required in both materials development and AM processing, for the printed composites to match the performance obtained with conventional composites.

Table 5: A comparison of interlaminar shear strength values obtained for unidirectional carbon and glass reinforced nylon parts, printed via material extrusion and an example of a current industry standard, fabricated via autoclave.

Fibre / Matrix	**Fabrication Method**	**Fibre Vol Fraction, vf (%)**	**Porosity (%)**	**ILSS (MPa)**
	3-D Printed			
Carbon / Nylon *(current study)*	Material Extrusion (Atmospheric)	41	6.8	43
Carbon / Nylon *(current study)*	Material Extrusion (Low-pressure)	41	1.1	58
Carbon / Nylon [9]	Material Extrusion (MarkTwo)	30 [(a)]	-	32
Glass / Nylon *(current study)*	Material Extrusion (Atmospheric)	35	1.5	39
Glass / Nylon *(current study)*	Material Extrusion (Low-pressure)	35	0.5	48
Glass / Nylon [9]	Material Extrusion (MarkTwo)	26 [(a)]	-	30

Kevlar / Nylon *(current study)*	Material Extrusion (Atmospheric)	35	2.5	28
Kevlar / Nylon *(current study)*	Material Extrusion (Low-pressure)	35	0.8	32
Kevlar / Nylon [9]	Material Extrusion (MarkTwo)	26 [(a)]	-	14
	Industry Standard			
Carbon / Epoxy [33] (HexPly®M91/34%/UD194/IM10-12K)	Autoclave, Unidirectional	59	-	105

(a) The V_f is calculated using the percentage prepreg filament reported in in Caminero and Chacón [9] and the 41% V_f in the carbon the 35% V_f in the glass and Kevlar prepreg filament.

4. Conclusions

In this study, for the first time, a low-pressure additive manufacturing technique was investigated for the fabrication of FRPC. Carbon, glass and Kevlar fibre reinforced nylon composite parts were printed both at atmospheric pressure, as well as in a vacuum chamber at 1 Pa. The impact of pressure on the both the porosity and interlaminar strength of the printed composites was investigated.

Prior to printing, the thermal properties of the filaments were evaluated based on DSC measurements. The glass and Kevlar nylon filaments exhibited a broad melting peak at 202 °C, a sharp recrystallisation during the cooling phase at 159 °C and contained 12 and 13% crystallinity, respectively. No melting peak was observed in the case of the carbon fibre nylon filament. From previous studies, this lack of DSC peak has been described previously as being associated with the thermal processing history of this polymer. Differences were also observed between the shape of the melting peaks observed for the glass and Kevlar fibre nylon filaments, which is also likely to be associated with the thermal processing history of nylon.

Under low pressure conditions, the carbon, glass and Kevlar reinforced printed parts exhibited a significant reduction in porosity of 5.7, 1.0 and 1.7 % respectively, compared with those printed at atmospheric pressure. A short beam shear test was used as a comparative method to compare the mechanical strength of the resulting composites. An increase in interlaminar shear strength of 33, 22 and 12% was observed for carbon, glass and Kevlar FRPC printed under low-pressure, compared to those printed under atmospheric pressure. The increase in mechanical strength is attributed to enhanced fibre-matrix bonding due to the reduction of voids in the prints. In addition, a comparison of shear strength values of similar, printed parts, indicates the capability of low-pressure AM, to fabricate parts with superior mechanical performance. While AM fabricated composites exhibit inferior mechanical

properties compared with high performance carbon epoxy laminates, the use of low-pressure processing has demonstrated considerable potential for enhancing the properties of AM fabricated composites.

Acknowledgements

This work was supported under both the SFI funded I-Form Advanced Manufacturing Research Centre – (16/RC/3872), and the MaREI SFI Centre for Marine Renewable Energy Research - (12/RC/2302). The authors would like to thank Dr. Saoirse Tracy, Director of the UCD X-ray CT facility at UCD Rosemount Experimental Research Station, for the use of scanner. Funding to purchase the X-ray μCT scanner was through a Science Foundation Ireland Infrastructure award (16/RI/3747).

Declaration of conflicting Interests

The authors declared no potential conflicts of interest with respect to the research, authorship and / or publication of this article.

References

1. Harris B. *Composite Materials* The Institute of Materials, London 1999.
2. Frketic J, Dickens T, Ramakrishnan S. Automated manufacturing and processing of fiber-reinforced polymer (FRP) composites: An additive review of contemporary and modern techniques for advanced materials manufacturing. *Additive Manufacturing.* 2017;14:69-86.
3. Wong KV, Hernandez A. A Review of Additive Manufacturing. *ISRN Mechanical Engineering.* 2012;2012:1-10.
4. Standards N. Additive manufacturing - General principles -Terminology (ISO/ASTM 52900:2015). *I.S. EN ISO/ASTM 52900:2017*2017.
5. Mohamed OA, Masood SH, Bhowmik JL. Optimization of fused deposition modeling process parameters: a review of current research and future prospects. *Advances in Manufacturing.* 2015;3(1):42-53.
6. Weihong Zhong FL, Zuoguang Zhang, Lulu Song, Zhimin Li. Short fiber reinforced composites for fused deposition modeling. *Materials Science and Engineering.* 2000(A301):125 - 130.
7. Ning F, Cong W, Qiu J, Wei J, Wang S. Additive manufacturing of carbon fiber reinforced thermoplastic composites using fused deposition modeling. *Composites Part B: Engineering.* 2015;80:369-378.
8. Nikzad M, Masood SH, Sbarski I. Thermo-mechanical properties of a highly filled polymeric composites for Fused Deposition Modeling. *Materials & Design.* 2011;32(6):3448-3456.
9. Caminero MA, Chacón JM, García-Moreno I, Reverte JM. Interlaminar bonding performance of 3D printed continuous fibre reinforced thermoplastic composites using fused deposition modelling. *Polymer Testing.* 2018;68:415-423.
10. Dickson AN, Barry JN, McDonnell KA, Dowling DP. Fabrication of continuous carbon, glass and Kevlar fibre reinforced polymer composites using additive manufacturing. *Additive Manufacturing.* 2017;16:146-152.
11. Hao W, Liu Y, Zhou H, Chen H, Fang D. Preparation and characterization of 3D printed continuous carbon fiber reinforced thermosetting composites. *Polymer Testing.* 2018;65:29-34.

12. Goh GD, Dikshit V, Nagalingam AP, et al. Characterization of mechanical properties and fracture mode of additively manufactured carbon fiber and glass fiber reinforced thermoplastics. *Materials & Design.* 2018;137:79-89.
13. Matsuzaki R, Ueda M, Namiki M, et al. Three-dimensional printing of continuous-fiber composites by in-nozzle impregnation. *Sci Rep.* 2016;6:23058.
14. Tian X, Liu T, Yang C, Wang Q, Li D. Interface and performance of 3D printed continuous carbon fiber reinforced PLA composites. *Composites Part A: Applied Science and Manufacturing.* 2016;88:198-205.
15. Bettini P, Alitta G, Sala G, Di Landro L. Fused Deposition Technique for Continuous Fiber Reinforced Thermoplastic. *Journal of Materials Engineering and Performance.* 2016;26(2):843-848.
16. Hu Q, Duan Y, Zhang H, Liu D, Yan B, Peng F. Manufacturing and 3D printing of continuous carbon fiber prepreg filament. *Journal of Materials Science.* 2017;53(3):1887-1898.
17. Chapiro M. Current achievements and future outlook for composites in 3D printing. *Reinforced Plastics.* 2016;60(6):372-375.
18. Justo J, Távara L, García-Guzmán L, París F. Characterization of 3D printed long fibre reinforced composites. *Composite Structures.* 2018;185:537-548.
19. Araya-Calvo M, López-Gómez I, Chamberlain-Simon N, et al. Evaluation of compressive and flexural properties of continuous fiber fabrication additive manufacturing technology. *Additive Manufacturing.* 2018;22:157-164.
20. Der Klift FV, Koga Y, Todoroki A, Ueda M, Hirano Y, Matsuzaki R. 3D Printing of Continuous Carbon Fibre Reinforced Thermo-Plastic (CFRTP) Tensile Test Specimens. *Open Journal of Composite Materials.* 2016;06(01):18-27.
21. Imeri A, Fidan I, Allen M, Wilson DA, Canfield S. Fatigue analysis of the fiber reinforced additively manufactured objects. *The International Journal of Advanced Manufacturing Technology*. 2018;98(9-12):2717-2724.
22. Mohammadizadeh M, Fidan I, Allen M, Imeri A. Creep behavior analysis of additively manufactured fiber-reinforced components. *The International Journal of Advanced Manufacturing Technology.* 2018.
23. Melenka GW, Cheung BKO, Schofield JS, Dawson MR, Carey JP. Evaluation and prediction of the tensile properties of continuous fiber-reinforced 3D printed structures. *Composite Structures.* 2016;153:866-875.
24. Sozer EM, Simacek P, Advani SG. Resin transfer molding (RTM) in polymer matrix composites. 2012:245-309.
25. Hubert P, Fernlund G, Poursartip A. Autoclave processing for composites. 2012:414-434.
26. O'Connor HJ, Dowling DP. Evaluation of the influence of low pressure additive manufacturing processing conditions on printed polymer parts. *Additive Manufacturing.* 2018;21:404-412.
27. 2344M ADD. Standard Test Method for Short-Beam Strength of Polymer Matrix Composite Materials and Their Laminates. 2000.
28. Y.Kong JNH. The measurement of the crystallinity of polymers by DSC. *Polymer* 2002;43:3873 - 3878.
29. V.P.Privalko TK, Yu.S.Lipatov. Crystallization of Filled Nylon 6. I. Heat Capacities and Melting Behavior *Polymer Journal* 1979;11(9):699 - 709
30. H.J.Whitford NACCa. How to Use the Two Sample t-Test. *Biometrical Journal.* 1986;28(2):131 - 148.
31. Zhen Mei, Chung DDL. Thermal history of carbon-fiber polymer-matrix composite, evaluated by electrical resistance measurement *Thermochimia Acta 369.* 2001:87-93.
32. Yin J, Lu C, Fu J, Huang Y, Zheng Y. Interfacial bonding during multi-material fused deposition modeling (FDM) process due to inter-molecular diffusion. *Materials & Design.* 2018;150:104-112.
33. Corporation H. *HexPly M91 Product Data Sheet.* https://www.hexcel.com/user_area/content_media/raw/HexPly_M91_global_DataSheet.pdf.